

The Topology of Chaos

Alice in Stretch and Squeezeland

Robert Gilmore

Marc Lefranc



A JOHN WILEY & SONS, INC., PUBLICATION

The page is intensely left blank

The Topology of Chaos

The page is intensely left blank

The Topology of Chaos

Alice in Stretch and Squeezeland

Robert Gilmore

Marc Lefranc



A JOHN WILEY & SONS, INC., PUBLICATION

This text is printed on acid-free paper. (2)

Copyright © 2002 by John Wiley & Sons, Inc., New York. All rights reserved.

Published simultaneously in Canada.

No part of this publication may be reproduced, stored in a retrieval system or transmitted in any form or by any means, electronic, mechanical, photocopying, recording, scanning or otherwise, except as permitted under Section 107 or 108 of the 1976 United States Copyright Act, without either the prior written permission of the Publisher, or authorization through payment of the appropriate per-copy fee to the Copyright Clearance Center, 222 Rosewood Drive, Danvers, MA 01923, (978) 750-8400, fax (978) 750-4744. Requests to the Publisher for permission should be addressed to the Permissions Department, John Wiley & Sons, Inc., 605 Third Avenue, New York, NY 10158-0012, (212) 850-6011, fax (212) 850-6008, E-Mail: PERMREQ @ WILEY.COM.

For ordering and customer service, call 1-800-CALL-WILEY.

Library of Congress Cataloging-in-Publication Data Is Available

ISBN 0-471-40816-6

Printed in the United States of America

10 9 8 7 6 5 4 3 2 1

Preface

Before the 1970s opportunities sometimes arose for physicists to study nonlinear systems. This was especially true in fields like fluid dynamics and plasma physics, where the fundamental equations are nonlinear and these nonlinearities masked (and still mask) the full spectrum of spectacularly rich behavior. When possible we avoided being dragged into the study of abstract nonlinear systems. For we believed, to paraphrase a beautiful generalization of Tolstoy, that

All linear systems are the same.

Each nonlinear system is nonlinear in its own way.

At that time we believed that one could spend a whole lifetime studying the nonlinearities of the van der Pol oscillator [Cartwright and Littlewood (1945), Levinson (1949)] and wind up knowing next to nothing about the behavior of the Duffing oscillator.

Nevertheless, other intrepid researchers had been making an assault on the complexities of nonlinear systems. Smale (1967) described a mechanism responsible for generating a great deal of the chaotic behavior which has been studied up to the present time. Lorenz, studying a drastic truncation of the Navier-Stokes equation, discovered and described 'sensitive dependence on initial conditions' (1963). The rigid order in which periodic orbits are created in the bifurcation set of the logistic map, and in fact any unimodal map of the interval to itself, was described by May (1976) and by Metropolis, Stein, and Stein (1973).

Still, There was a reluctance on the part of most scientists to indulge in the study of nonlinear systems.

This all changed with Feigenbaum's discoveries (1978). He showed that scaling invariance in period doubling cascades leads to quantitative (later, qualitative) predictions. These are the scaling ratios

$$\begin{aligned}\delta &= 4.66920\ 16091\ 029 \cdots && \text{control parameter space} \\ \alpha &= -2.50290\ 78750\ 959 \cdots && \text{state variable space}\end{aligned}$$

which are eigenvalues of a renormalization transformation. The transformation in the attitude of scientists is summarized by the statement (Gleick, 1987)

"It was a very happy and shocking discovery that there were structures in nonlinear systems that are always the same if you looked at them the right way."

This discovery launched an avalanche of work on nonlinear dynamical systems. Old experiments, buried and forgotten because of instabilities or unrepeatability due to incompetent graduate students (in their advisor's opinions) were resurrected and pushed as ground-breaking experiments exhibiting 'first observations' of chaotic behavior (by these same advisors). And many new experiments were carried out, at first to test Feigenbaum's scaling predictions, then to test other quantitative predictions, then just to see what would happen.

Some of the earliest experiments were done on fluids, since the fundamental equations are known and are nonlinear. However, these experiments often suffered from the long time scales (days, weeks, or months) required to record a decent data set. Oscillating chemical reactions (e.g., the Belousov-Zhabotinskii reaction) yielded a wide spectrum of periodic and chaotic behavior which was relatively easy to control and to tune. These data sets could be generated in hours or days. Nonlinear electric circuits were also extensively studied, although there was (and still is) a prejudice to regard them with a jaundiced eye as little more than analog computers. Such data sets could be generated very quickly (seconds to minutes) — almost as fast as numerical simulations. Finally, laser laboratories contributed in a substantial way to build up extensive and widely varying data banks very quickly (milleseconds to minutes) of chaotic data.

It was at this time (1988), about 10 years into the 'nonlinear science' revolution, that one of the authors (RG) was approached by his colleague (J. R. Tredicce, then at Drexel, now at the Institut Non Linéaire de Nice) with the proposition: "Bob, can you help me explain my data?" (See Chapter 1). So we swept the accumulated clutter off my desk and deposited his data. We looked, pushed, probed, discussed, studied, ... for quite a while. Finally, I replied: "No." Tredicce left with his data. But he is very smart (he is an experimentalist!), and returned the following day with the same pile of stuff. The conversation was short and effective: "Bob," "Still my name," "I'll bet that you *can't* explain my data." (Bob sees red!) We sat down and discussed further. At the time two tools were available for studying chaotic data. These involved estimating Lyapunov exponents (dynamical stability) and estimating fractal dimension (geometry). Both required lots of very clean data and long calculations. They provided real number(s) with no convincing error bars, no underlying statistical theory, and no independent way to verify these guesses. And at the end of the day neither provided any information on "how to model the dynamics."

Even worse: before doing an analysis I would like to know what I am looking for, or at least know what the spectrum of possible results looks like. For example, when we analyze chemical elements or radionuclides, there is a Periodic Table of the Chemical Elements and another for the Atomic Nuclei which accommodate any such analyses. At that time, no classification theory existed for strange attractors.

In response to Tredicce's dare, I promised to (try to) analyze his data. But I pointed out that a serious analysis couldn't be done until we first had some handle on the classification of strange attractors. This could take a long time. Tredicce promised to be patient. And he was.

Our first step was to consider the wisdom of Poincaré. He suggested about a century earlier that one could learn a great deal about the behavior of nonlinear systems by studying their unstable periodic orbits which

"... yield us the solutions so precious, that is to say, they are the only breach through which we can penetrate into a place which up to now has been reputed to be inaccessible."

This observation was compatible with what we learned from experimental data: the most important features that governed the behavior of a system, and especially that governed the perestroikas of such systems (i.e., changes as control parameters are changed) are the features that you can't see — the unstable periodic orbits.

Accordingly, my colleagues and I studied the invariants of periodic orbits, their (Gauss) linking numbers. We also introduced a refined topological invariant based on periodic orbits — the relative rotation rates (Chapter 4). Finally, we used these invariants to identify topological structures (branched manifolds or templates, Chapter 5) which we used to classify strange attractors "in the large." The result was that "low dimensional" strange attractors (i.e., those that could be embedded in three-dimensional spaces) could be classified. This classification depends on the periodic orbits "in" the strange attractor, in particular, on their organization as elicited by their invariants. The classification is topological. That is, it is given by a set of integers (also by very informative pictures). Not only that, these integers can be extracted from experimental data. The data sets do not have to be particularly long or particularly clean — especially by fractal dimension calculation standards. Further, there are built in internal self-consistency checks. That is, the topological analysis algorithm (Chapter 6) comes with reject/fail to reject test criteria. This is the first — and remains the only — chaotic data analysis procedure with rejection criteria.

Ultimately we discovered, through analysis of experimental data, that there is a secondary, more refined classification for strange attractors. This depends on a "basis set of orbits" which describes the spectrum of all the unstable periodic orbits "in" a strange attractor (Chapter 9).

The ultimate result is a doubly discrete classification of strange attractors. Both parts of this doubly discrete classification depend on unstable periodic orbits. The classification depends on identifying:

Branched Manifold - which describes the stretching and squeezing mechanisms that operate repetitively on a flow in phase space to build up a (hyperbolic) strange attractor and to organize all the unstable periodic orbits in the strange

attractor in a unique way. The branched manifold is identified by the spectrum of the invariants of the periodic orbits that it supports.

Basis Set of Orbits - which describes the spectrum of unstable period orbits in a (nonhyperbolic) strange attractor.

The perestroikas of branched manifolds and of basis sets of orbits in this doubly discrete classification obey well-defined topological constraints. These constraints provide both a rigidity and a flexibility for the evolution of strange attractors as control parameters are varied.

Along the way we discovered that dynamical systems with symmetry can be related to dynamical systems without symmetry in very specific ways (Chapter 10). As usual, these relations involve both a rigidity and a flexibility which is as surprising as it is delightful.

Many of these insights are described in the paper *Topological analysis of chaotic dynamical systems*, *Reviews of Modern Physics*, 70(4), 1455-1530 (1998), which forms the basis for part of this book. We thank the editors of this journal for their policy of encouraging transformation of research articles to longer book format.

The encounter (fall in love?) of the other author (M.L.) with topological analysis dates back to 1991, when he was a PhD student at the University of Lille, struggling to extract information from the very same type of chaotic laser that Tredicce was using. At that time, Marc was computing estimates of fractal dimensions for his laser. But they depended very much on the coordinate system used and gave no insight into the mechanisms responsible for chaotic behavior, even less into the succession of the different behaviors observed. This was very frustrating. There had been this very intriguing paper in *Physical Review Letters* about a "Characterization of strange attractors by integers", with appealing ideas and nice pictures. But as with many short papers, it had been difficult to understand how you should proceed when faced with a real experimental system. Topological analysis struck back when Pierre Glorieux, then Marc's advisor, came back to Lille from a stay in Philadelphia, and handed him a preprint from the Drexel team, saying: "You should have a look at this stuff". The preprint was about topological analysis of the Belousov-Zhabotinskii reaction, a real-life system. It was the Rosetta Stone that helped put pieces together. Soon after, pictures of braids constructed from laser signals were piling up on the desk. They were absolutely identical to those extracted from the Belousov-Zhabotinskii data and described in the preprint. There was universality in chaos if you looked at it with the right tools. Eventually, the system that had motivated topological analysis in Philadelphia, the CO₂ laser with modulated losses, was characterized in Lille and shown to be described by a horseshoe template. Indeed, Tredicce's laser could not be characterized by topological analysis because of long periods of zero output intensity that prevented invariants from being reliably estimated. The high signal to noise ratio of the laser in Lille allowed us to use a logarithmic amplifier and to resolve the structure of trajectories in the zero intensity region.

But a classification is only useful if there exist different classes. Thus, one of the early goals was to find experimental evidence of a topological organization that would differ from the standard Smale's horseshoe. At that time, some regimes of the

modulated CO₂ laser could not be analyzed for lack of a suitable symbolic encoding. The corresponding Poincaré sections had peculiar structures that, depending on the observer's mood, suggested a doubly iterated horseshoe or an underlying three-branch manifold. Since the complete analysis could not be carried out, much time was spent on trying to find at least one orbit that could not fit the horseshoe template. The result was extremely disappointing: For every orbit detected, there was at least one horseshoe orbit with identical invariants. One of the most important lessons of Judo is that if you experience resistance when pushing, you should pull (and vice versa). Similarly, this failed attempt to find a nonhorseshoe template turned into techniques to determine underlying templates when no symbolic coding is available and to construct such codings using the information extracted from topological invariants.

But the search for different templates was not over. Two of Marc's colleagues, Dominique Derozier and Serge Bielawski, proposed for him to study a fiber laser they had in their laboratory (that was the perfect system to study knots). This system exhibits chaotic tongues when the modulation frequency is near a subharmonic of its relaxation frequency: It was tempting to check whether the topological structures in each tongue differed. That was indeed the case: The corresponding templates were basically horseshoe templates but with a global torsion increasing systematically from one tongue to the other. A Nd:YAG laser was also investigated. It showed similar behavior, until the day where Guillaume Boulant, the PhD student working on the laser, came to Marc's office and said: "I have a weird data set". Chaotic attractors were absolutely normal, return maps resembled the logistic map very much, but the invariants were simply not what we were used to. This was the first evidence of a reverse horseshoe attractor. How topological organizations are modified as a control parameter is varied was the subject of many discussions in Lille in the following months, a rather accurate picture finally emerged and papers began to be written. In the last stages, Marc did a bibliographic search just to clear his mind and... a recent 22-page Physical Review paper, by McCallum and Gilmore, turned up. Even though it was devoted to the Duffing attractor, it described with great detail what was happening in our lasers as control parameters are modified. Every occurrence of "We conjecture that" in the papers was hastily replaced by "Our experiments confirm the theoretical prediction...", and papers were sent to Physical Review. They were accepted 15 days later, with a very positive review. Soon after, the Referee contacted us and proposed a joint effort on extensions of topological analysis. The Referee was Bob, and this was the start of a collaboration that we hope will last long.

It would indeed be very nice if these techniques could be extended to the analysis of strange attractors in higher dimensions (than three). Such an extension, if it is possible, cannot rely on the most powerful tools available in three dimensions. These are the topological invariants used to tease out information on how periodic orbits are organized in a strange attractor. We cannot use these tools (linking numbers, relative rotation rates) because knots "fall apart" in higher dimensions. We explore (Chapter 11) an inviting possibility for studying an important class of strange attractors in four dimensions. If a classification procedure based on these methods is successful, the door is opened to classifying strange attractors in R^n , $n > 3$. A number of ideas that

may be useful in this effort have already proved useful in two closely-related fields (Chapter 12): Lie group theory and singularity theory.

Some of the highly technical details involved in extracting templates from data have been archived in the appendix. Other technical matter is archived at our web sites.¹

Much of the early work in this field was done in response to the challenge by J. R. Tredicce and carried out with my colleagues and close friends: H. G. Solari, G. B. Mindlin, N. B. Tuffillaro, F. Papoff, and R. Lopez-Ruiz. Work on symmetries was done with C. Letellier. Part of the work carried out in this program has been supported by the National Science Foundation under grants NSF 8843235 and NSF 9987468. Similarly, Marc would like to thank colleagues and students with whom he enjoyed working and exchanging ideas about topological analysis: Pierre Glorieux, Ennio Arimondo, Francesco Papoff, Serge Bielawski, Dominique Derozier, Guillaume Boulant, and Jérôme Plumecoq. Stays of Bob in Lille were partially funded by the University of Lille, the Centre National de la Recherche Scientifique, Drexel University under sabbatical leave, and by the NSF.

Last and most important, we thank our wives Claire and Catherine for their warm encouragement while physics danced in our heads, and our children, Marc and Keith, Clara and Martin, who competed with our research and demanded our attention, and by doing so, kept us human.

R.G. AND M.L.

Lille, France, Jan. 2002

¹<http://einstein.drexel.edu/directory/faculty/Gilmore.html> and <http://www.phlam.univ-lille1.fr/perso/lefranc.html>

Contents

<i>Preface</i>	v
1 Introduction	1
1.1 <i>Laser with Modulated Losses</i>	2
1.2 <i>Objectives of a New Analysis Procedure</i>	10
1.3 <i>Preview of Results</i>	11
1.4 <i>Organization of This Work</i>	12
2 Discrete Dynamical Systems: Maps	17
2.1 <i>Introduction</i>	17
2.2 <i>Logistic Map</i>	19
2.3 <i>Bifurcation Diagrams</i>	21
2.4 <i>Elementary Bifurcations in the Logistic Map</i>	23
2.4.1 <i>Saddle-Node Bifurcation</i>	23
2.4.2 <i>Period-Doubling Bifurcation</i>	27
2.5 <i>Map Conjugacy</i>	30
2.5.1 <i>Changes of Coordinates</i>	30
2.5.2 <i>Invariants of Conjugacy</i>	31
	xi

2.6	<i>Fully Developed Chaos in the Logistic Map</i>	32
2.6.1	<i>Iterates of the Tent Map</i>	33
2.6.2	<i>Lyapunov Exponents</i>	35
2.6.3	<i>Sensitivity to Initial Conditions and Mixing</i>	35
2.6.4	<i>Chaos and Density of (Unstable) Periodic Orbits</i>	36
2.6.5	<i>Symbolic Coding of Trajectories: First Approach</i>	38
2.7	<i>One-Dimensional Symbolic Dynamics</i>	40
2.7.1	<i>Partitions</i>	40
2.7.2	<i>Symbolic Dynamics of Expansive Maps</i>	43
2.7.3	<i>Grammar of Chaos: First Approach</i>	46
2.7.4	<i>Kneading Theory</i>	49
2.7.5	<i>Bifurcation Diagram of the Logistic Map Revisited</i>	53
2.8	<i>Shift Dynamical Systems, Markov Partitions, and Entropy</i>	57
2.8.1	<i>Shifts of Finite Type and Topological Markov Chains</i>	57
2.8.2	<i>Periodic Orbits and Topological Entropy of a Markov Chain</i>	59
2.8.3	<i>Markov Partitions</i>	61
2.8.4	<i>Approximation by Markov Chains</i>	62
2.8.5	<i>Zeta Function</i>	63
2.8.6	<i>Dealing with Grammars</i>	64
2.9	<i>Fingerprints of Periodic Orbits and Orbit Forcing</i>	67
2.9.1	<i>Permutation of Periodic Points as a Topological Invariant</i>	67
2.9.2	<i>Topological Entropy of a Periodic Orbit</i>	69
2.9.3	<i>Period-3 Implies Chaos and Sarkovskii's Theorem</i>	71
2.9.4	<i>Period-3 Does Not Always Imply Chaos: Role of Phase-Space Topology</i>	72
2.9.5	<i>Permutations and Orbit Forcing</i>	72
2.10	<i>Two-Dimensional Dynamics: Smale's Horseshoe</i>	74

2.10.1	<i>Horseshoe Map</i>	74
2.10.2	<i>Symbolic Dynamics of the Invariant Set</i>	75
2.10.3	<i>Dynamical Properties</i>	78
2.10.4	<i>Variations on the Horseshoe Map: Baker Maps</i>	79
2.11	<i>Hénon Map</i>	82
2.11.1	<i>A Once-Folding Map</i>	82
2.11.2	<i>Symbolic Dynamics of the Hénon Map</i>	84
2.12	<i>Circle Maps</i>	90
2.12.1	<i>A New Global Topology</i>	90
2.12.2	<i>Frequency Locking and Arnol'd Tongues</i>	91
2.12.3	<i>Chaotic Circle Maps and Annulus Maps</i>	94
2.13	<i>Summary</i>	95
3	<i>Continuous Dynamical Systems: Flows</i>	97
3.1	<i>Definition of Dynamical Systems</i>	97
3.2	<i>Existence and Uniqueness Theorem</i>	98
3.3	<i>Examples of Dynamical Systems</i>	99
3.3.1	<i>Duffing Equation</i>	99
3.3.2	<i>van der Pol Equation</i>	100
3.3.3	<i>Lorenz Equations</i>	102
3.3.4	<i>Rössler Equations</i>	105
3.3.5	<i>Examples of Nondynamical Systems</i>	106
3.3.6	<i>Additional Observations</i>	109
3.4	<i>Change of Variables</i>	112
3.4.1	<i>Diffeomorphisms</i>	112
3.4.2	<i>Examples</i>	112
3.4.3	<i>Structure Theory</i>	114
3.5	<i>Fixed Points</i>	116
3.5.1	<i>Dependence on Topology of Phase Space</i>	116
3.5.2	<i>How to Find Fixed Points in R^n</i>	117
3.5.3	<i>Bifurcations of Fixed Points</i>	118
3.5.4	<i>Stability of Fixed Points</i>	120
3.6	<i>Periodic Orbits</i>	121
3.6.1	<i>Locating Periodic Orbits in $R^{n-1} \times S^1$</i>	121

3.6.2	<i>Bifurcations of Fixed Points</i>	122
3.6.3	<i>Stability of Fixed Points</i>	123
3.7	<i>Flows near Nonsingular Points</i>	124
3.8	<i>Volume Expansion and Contraction</i>	125
3.9	<i>Stretching and Squeezing</i>	126
3.10	<i>The Fundamental Idea</i>	127
3.11	<i>Summary</i>	128
4	<i>Topological Invariants</i>	131
4.1	<i>Stretching and Squeezing Mechanisms</i>	132
4.2	<i>Linking Numbers</i>	136
4.2.1	<i>Definitions</i>	136
4.2.2	<i>Reidemeister Moves</i>	138
4.2.3	<i>Braids</i>	139
4.2.4	<i>Examples</i>	142
4.2.5	<i>Linking Numbers for the Horseshoe</i>	143
4.2.6	<i>Linking Numbers for the Lorenz Attractor</i>	144
4.2.7	<i>Linking Numbers for the Period-Doubling Cascade</i>	146
4.2.8	<i>Local Torsion</i>	146
4.2.9	<i>Writhe and Twist</i>	147
4.2.10	<i>Additional Properties</i>	148
4.3	<i>Relative Rotation Rates</i>	149
4.3.1	<i>Definition</i>	150
4.3.2	<i>How to Compute Relative Rotation Rates</i>	151
4.3.3	<i>Horseshoe Mechanism</i>	155
4.3.4	<i>Additional Properties</i>	159
4.4	<i>Relation between Linking Numbers and Relative Rotation Rates</i>	159
4.5	<i>Additional Uses of Topological Invariants</i>	160
4.5.1	<i>Bifurcation Organization</i>	160
4.5.2	<i>Torus Orbits</i>	161
4.5.3	<i>Additional Remarks</i>	161
4.6	<i>Summary</i>	164

5	<i>Branched Manifolds</i>	165
5.1	<i>Closed Loops</i>	166
5.1.1	<i>Undergraduate Students</i>	166
5.1.2	<i>Graduate Students</i>	166
5.1.3	<i>The Ph.D. Candidate</i>	166
5.1.4	<i>Important Observation</i>	168
5.2	<i>What Has This Got to Do with Dynamical Systems?</i>	169
5.3	<i>General Properties of Branched Manifolds</i>	169
5.4	<i>Birman–Williams Theorem</i>	171
5.4.1	<i>Birman–Williams Projection</i>	171
5.4.2	<i>Statement of the Theorem</i>	173
5.5	<i>Relaxation of Restrictions</i>	175
5.5.1	<i>Strongly Contracting Restriction</i>	175
5.5.2	<i>Hyperbolic Restriction</i>	176
5.6	<i>Examples of Branched Manifolds</i>	176
5.6.1	<i>Smale–Rössler System</i>	177
5.6.2	<i>Lorenz System</i>	179
5.6.3	<i>Duffing System</i>	180
5.6.4	<i>van der Pol System</i>	182
5.7	<i>Uniqueness and Nonuniqueness</i>	186
5.7.1	<i>Local Moves</i>	186
5.7.2	<i>Global Moves</i>	187
5.8	<i>Standard Form</i>	190
5.9	<i>Topological Invariants</i>	193
5.9.1	<i>Kneading Theory</i>	193
5.9.2	<i>Linking Numbers</i>	197
5.9.3	<i>Relative Rotation Rates</i>	198
5.10	<i>Additional Properties</i>	199
5.10.1	<i>Period as Linking Number</i>	199
5.10.2	<i>EBK–like Expression for Periods</i>	199
5.10.3	<i>Poincaré Section</i>	201
5.10.4	<i>Blow-Up of Branched Manifolds</i>	201
5.10.5	<i>Branched-Manifold Singularities</i>	203
5.10.6	<i>Constructing a Branched Manifold from a Map</i>	203

5.10.7	<i>Topological Entropy</i>	203
5.11	<i>Subtemplates</i>	207
5.11.1	<i>Two Alternatives</i>	207
5.11.2	<i>A Choice</i>	210
5.11.3	<i>Topological Entropy</i>	211
5.11.4	<i>Subtemplates of the Smale Horseshoe</i>	212
5.11.5	<i>Subtemplates Involving Tongues</i>	213
5.12	<i>Summary</i>	215
6	<i>Topological Analysis Program</i>	217
6.1	<i>Brief Summary of the Topological Analysis Program</i>	217
6.2	<i>Overview of the Topological Analysis Program</i>	218
6.2.1	<i>Find Periodic Orbits</i>	218
6.2.2	<i>Embed in \mathbb{R}^3</i>	220
6.2.3	<i>Compute Topological Invariants</i>	220
6.2.4	<i>Identify Template</i>	221
6.2.5	<i>Verify Template</i>	222
6.2.6	<i>Model Dynamics</i>	223
6.2.7	<i>Validate Model</i>	224
6.3	<i>Data</i>	225
6.3.1	<i>Data Requirements</i>	225
6.3.2	<i>Processing in the Time Domain</i>	226
6.3.3	<i>Processing in the Frequency Domain</i>	228
6.4	<i>Embeddings</i>	233
6.4.1	<i>Embeddings for Periodically Driven Systems</i>	234
6.4.2	<i>Differential Embeddings</i>	235
6.4.3	<i>Differential–Integral Embeddings</i>	237
6.4.4	<i>Embeddings with Symmetry</i>	238
6.4.5	<i>Time–Delay Embeddings</i>	239
6.4.6	<i>Coupled–Oscillator Embeddings</i>	241
6.4.7	<i>SVD Projections</i>	242
6.4.8	<i>SVD Embeddings</i>	244
6.4.9	<i>Embedding Theorems</i>	244
6.5	<i>Periodic Orbits</i>	246

6.5.1	<i>Close Returns Plots for Flows</i>	246
6.5.2	<i>Close Returns in Maps</i>	249
6.5.3	<i>Metric Methods</i>	250
6.6	<i>Computation of Topological Invariants</i>	251
6.6.1	<i>Embed Orbits</i>	251
6.6.2	<i>Linking Numbers and Relative Rotation Rates</i>	252
6.6.3	<i>Label Orbits</i>	252
6.7	<i>Identify Template</i>	252
6.7.1	<i>Period-1 and Period-2 Orbits</i>	252
6.7.2	<i>Missing Orbits</i>	253
6.7.3	<i>More Complicated Branched Manifolds</i>	253
6.8	<i>Validate Template</i>	253
6.8.1	<i>Predict Additional Topological Invariants</i>	254
6.8.2	<i>Compare</i>	254
6.8.3	<i>Global Problem</i>	254
6.9	<i>Model Dynamics</i>	254
6.10	<i>Validate Model</i>	257
6.10.1	<i>Qualitative Validation</i>	257
6.10.2	<i>Quantitative Validation</i>	258
6.11	<i>Summary</i>	259
7	<i>Folding Mechanisms: A_2</i>	261
7.1	<i>Belousov–Zhabotinskii Chemical Reaction</i>	262
7.1.1	<i>Location of Periodic Orbits</i>	262
7.1.2	<i>Embedding Attempts</i>	266
7.1.3	<i>Topological Invariants</i>	267
7.1.4	<i>Template</i>	271
7.1.5	<i>Dynamical Properties</i>	271
7.1.6	<i>Models</i>	273
7.1.7	<i>Model Verification</i>	273
7.2	<i>Laser with Saturable Absorber</i>	275
7.2.1	<i>Experimental Setup</i>	275
7.2.2	<i>Data</i>	276
7.2.3	<i>Topological Analysis</i>	276

7.2.4	<i>Useful Observation</i>	278
7.2.5	<i>Important Conclusion</i>	278
7.3	<i>Stringed Instrument</i>	279
7.3.1	<i>Experimental Arrangement</i>	279
7.3.2	<i>Flow Models</i>	280
7.3.3	<i>Dynamical Tests</i>	281
7.3.4	<i>Topological Analysis</i>	282
7.4	<i>Lasers with Low-Intensity Signals</i>	284
7.4.1	<i>SVD Embedding</i>	286
7.4.2	<i>Template Identification</i>	286
7.4.3	<i>Results of the Analysis</i>	288
7.5	<i>The Lasers in Lille</i>	288
7.5.1	<i>Class B Laser Model</i>	289
7.5.2	<i>CO₂ Laser with Modulated Losses</i>	295
7.5.3	<i>Nd-Doped YAG Laser</i>	300
7.5.4	<i>Nd-Doped Fiber Laser</i>	303
7.5.5	<i>Synthesis of Results</i>	308
7.6	<i>Neuron with Subthreshold Oscillations</i>	315
7.7	<i>Summary</i>	321
8	<i>Tearing Mechanisms: A₃</i>	323
8.1	<i>Lorenz Equations</i>	324
8.1.1	<i>Fixed Points</i>	325
8.1.2	<i>Stability of Fixed Points</i>	325
8.1.3	<i>Bifurcation Diagram</i>	325
8.1.4	<i>Templates</i>	326
8.1.5	<i>Shimizu–Morioka Equations</i>	328
8.2	<i>Optically Pumped Molecular Laser</i>	329
8.2.1	<i>Models</i>	331
8.2.2	<i>Amplitudes</i>	332
8.2.3	<i>Template</i>	333
8.2.4	<i>Orbits</i>	333
8.2.5	<i>Intensities</i>	337
8.3	<i>Fluid Experiments</i>	338

8.3.1	<i>Data</i>	340
8.3.2	<i>Template</i>	340
8.4	<i>Why A_3?</i>	341
8.5	<i>Summary</i>	341
9	<i>Unfoldings</i>	343
9.1	<i>Catastrophe Theory as a Model</i>	344
9.1.1	<i>Overview</i>	344
9.1.2	<i>Example</i>	344
9.1.3	<i>Reduction to a Germ</i>	346
9.1.4	<i>Unfolding the Germ</i>	348
9.1.5	<i>Summary of Concepts</i>	348
9.2	<i>Unfolding of Branched Manifolds: Branched Manifolds as Germs</i>	348
9.2.1	<i>Unfolding of Folds</i>	349
9.2.2	<i>Unfolding of Tears</i>	350
9.3	<i>Unfolding within Branched Manifolds: Unfolding of the Horseshoe</i>	351
9.3.1	<i>Topology of Forcing: Maps</i>	352
9.3.2	<i>Topology of Forcing: Flows</i>	352
9.3.3	<i>Forcing Diagrams</i>	355
9.3.4	<i>Basis Sets of Orbits</i>	361
9.3.5	<i>Coexisting Basins</i>	362
9.4	<i>Missing Orbits</i>	362
9.5	<i>Routes to Chaos</i>	363
9.6	<i>Summary</i>	365
10	<i>Symmetry</i>	367
10.1	<i>Information Loss and Gain</i>	368
10.1.1	<i>Information Loss</i>	368
10.1.2	<i>Exchange of Symmetry</i>	368
10.1.3	<i>Information Gain</i>	368
10.1.4	<i>Symmetries of the Standard Systems</i>	368
10.2	<i>Cover and Image Relations</i>	369

10.2.1	<i>General Setup</i>	369
10.3	<i>Rotation Symmetry 1: Images</i>	370
10.3.1	<i>Image Equations and Flows</i>	370
10.3.2	<i>Image of Branched Manifolds</i>	373
10.3.3	<i>Image of Periodic Orbits</i>	374
10.4	<i>Rotation Symmetry 2: Covers</i>	376
10.4.1	<i>Topological Index</i>	376
10.4.2	<i>Covers of Branched Manifolds</i>	378
10.4.3	<i>Covers of Periodic Orbits</i>	380
10.5	<i>Peeling: A New Global Bifurcation</i>	380
10.5.1	<i>Orbit Perestroika</i>	381
10.5.2	<i>Covering Equations</i>	382
10.6	<i>Inversion Symmetry: Driven Oscillators</i>	383
10.6.1	<i>Periodically Driven Nonlinear Oscillator</i>	384
10.6.2	<i>Embedding in $M^3 \subset R^4$</i>	384
10.6.3	<i>Symmetry Reduction</i>	385
10.6.4	<i>Image Dynamics</i>	385
10.7	<i>Duffing Oscillator</i>	386
10.8	<i>van der Pol Oscillator</i>	389
10.9	<i>Summary</i>	395
11	<i>Flows in Higher Dimensions</i>	397
11.1	<i>Review of Classification Theory in R^3</i>	397
11.2	<i>General Setup</i>	399
11.2.1	<i>Spectrum of Lyapunov Exponents</i>	400
11.2.2	<i>Double Projection</i>	400
11.3	<i>Flows in R^4</i>	402
11.3.1	<i>Cyclic Phase Spaces</i>	402
11.3.2	<i>Floppiness and Rigidity</i>	402
11.3.3	<i>Singularities in Return Maps</i>	404
11.4	<i>Cusp Bifurcation Diagrams</i>	406
11.4.1	<i>Cusp Return Maps</i>	408
11.4.2	<i>Structure in the Control Plane</i>	408
11.4.3	<i>Comparison with the Fold</i>	409

11.5	<i>Nonlocal Singularities</i>	411
11.5.1	<i>Multiple Cusps</i>	411
11.5.2	<i>Cusps and Folds</i>	413
11.6	<i>Global Boundary Conditions</i>	414
11.6.1	<i>R^1 and S^1 in Three-Dimensional Flows</i>	415
11.6.2	<i>Compact Connected Two-Dimensional Domains</i>	415
11.6.3	<i>Singularities in These Domains</i>	416
11.6.4	<i>Compact Connected Two-Dimensional Domains</i>	416
11.7	<i>Summary</i>	418
12	<i>Program for Dynamical Systems Theory</i>	421
12.1	<i>Reduction of Dimension</i>	422
12.1.1	<i>Absorbing Manifold</i>	424
12.1.2	<i>Inertial Manifold</i>	424
12.1.3	<i>Branched Manifolds</i>	424
12.2	<i>Equivalence</i>	425
12.2.1	<i>Diffeomorphisms</i>	425
12.3	<i>Structure Theory</i>	426
12.3.1	<i>Reducibility of Dynamical Systems</i>	426
12.4	<i>Germ</i>	427
12.4.1	<i>Branched Manifolds</i>	427
12.4.2	<i>Singular Return Maps</i>	427
12.5	<i>Unfolding</i>	428
12.6	<i>Paths</i>	430
12.6.1	<i>Routes to Chaos</i>	430
12.7	<i>Rank</i>	431
12.7.1	<i>Stretching and Squeezing</i>	431
12.8	<i>Complex Extensions</i>	432
12.8.1	<i>Fixed-Point Distributions</i>	432
12.8.2	<i>Singular Return Maps</i>	432
12.9	<i>Coxeter–Dynkin Diagrams</i>	433
12.9.1	<i>Fixed-Point Distributions</i>	433

12.9.2	<i>Singular Return Maps</i>	433
12.10	<i>Real Forms</i>	434
12.10.1	<i>Stability of Fixed Points</i>	434
12.10.2	<i>Singular Return Maps</i>	435
12.11	<i>Local vs. Global Classification</i>	436
12.11.1	<i>Nonlocal Folds</i>	436
12.11.2	<i>Nonlocal Cusps</i>	436
12.12	<i>Cover–Image Relations</i>	437
12.13	<i>Symmetry Breaking and Restoration</i>	437
12.13.1	<i>Entrainment and Synchronization</i>	437
12.14	<i>Summary</i>	439
<i>Appendix A Determining Templates from Topological Invariants</i>		441
A.1	<i>The Fundamental Problem</i>	441
A.2	<i>From Template Matrices to Topological Invariants</i>	443
A.2.1	<i>Classification of Periodic Orbits by Symbolic Names</i>	443
A.2.2	<i>Algebraic Description of a Template</i>	444
A.2.3	<i>Local Torsion</i>	445
A.2.4	<i>Relative Rotation Rates: Examples</i>	446
A.2.5	<i>Relative Rotation Rates: General Case</i>	448
A.3	<i>Identifying Templates from Invariants</i>	452
A.3.1	<i>Using an Independent Symbolic Coding</i>	452
A.3.2	<i>Simultaneous Determination of Symbolic Names and Template</i>	455
A.4	<i>Constructing Generating Partitions</i>	459
A.4.1	<i>Symbolic Encoding as an Interpolation Process</i>	459
A.4.2	<i>Generating partitions for Experimental Data</i>	463
A.4.3	<i>Comparison with Methods Based on Homoclinic Tangencies</i>	464
A.4.4	<i>Symbolic Dynamics on Three Symbols</i>	466
A.5	<i>Summary</i>	467

References **469**

Topic Index **483**

The page is intensely left blank

1

Introduction

1.1 Laser with Modulated Losses	2
1.3 Objectives of a New Analysis Procedure	10
1.3 Preview of Results	11
1.4 Organization of This Work	12

The subject of this book is the analysis of data generated by a dynamical system operating in a chaotic regime. More specifically, we describe how to extract, from chaotic data, topological signatures that determine the stretching and squeezing mechanisms which act on flows in phase space and which are responsible for generating chaotic data.

In the first section of this introductory chapter we describe, for purposes of motivation, a laser that has been operated under conditions in which it behaved chaotically. The topological methods of analysis that we describe in this book were developed in response to the challenge of analyzing chaotic data sets generated by this laser.

In the second section we list a number of questions which we would like to be able to answer when analyzing a chaotic signal. None of these questions can be addressed by the older tools for analyzing chaotic data: estimates of the spectrum of Lyapunov exponents and estimates of the spectrum of fractal dimensions. The question that we would particularly like to be able to answer is this: How does one model the dynamics? To answer this question we must determine the stretching and squeezing mechanisms that operate together—repeatedly—to generate chaotic data. The stretching mechanism is responsible for *sensitivity to initial conditions* while the squeezing mechanism is responsible for *recurrent nonperiodic behavior*. These

two mechanisms operate repeatedly to generate a strange attractor with a self-similar structure.

A new analysis method, topological analysis, has been developed to respond to the fundamental question just stated [1,2]. At the present time this method is suitable only for strange attractors that can be embedded in three-dimensional spaces. However, for such strange attractors it offers a complete and satisfying resolution to this question. The results are previewed in the third section of this chapter. In the final section we provide a brief overview of the organization of this book. In particular, we summarize the organization and content of the following chapters.

It is astonishing that the topological analysis tools that we describe have provided answers to more questions than we asked originally. This analysis procedure has also raised more questions than we have answered. We hope that the interaction between experiment and theory and between old questions answered and new questions raised will hasten evolution of the field of nonlinear dynamics.

1.1 LASER WITH MODULATED LOSSES

The possibility of observing chaos in lasers was originally demonstrated by Arecchi et al. [3] and by Gioggia and Abraham [4]. The use of lasers as a testbed for generating deterministic chaotic signals has two major advantages over fluid and chemical systems, which until that time had been the principal sources for chaotic data:

1. The time scales intrinsic to a laser (10^{-7} to 10^{-3} s) are much shorter than the time scales in fluid experiments and oscillating chemical reactions. This is important for experimentalists, since it is possible to explore a very large parameter range during a relatively short time.
2. Reliable laser models exist in terms of a small number of ordinary differential equations whose solutions show close qualitative similarity to the behavior of the lasers that are modeled [5, 6].

The topological methods described in the remainder of this work were originally developed to understand the data generated by a laser with modulated losses [6]. A schematic of this laser is shown in Fig. 1.1. A CO₂ gas tube is placed between two infrared mirrors (M). The ends of the tube are terminated by Brewster angle windows, which polarize the field amplitude in the vertical direction. Under normal operating conditions, the laser is very stable. A Kerr cell (K) is placed inside the laser cavity. The Kerr cell modifies the polarization state of the electromagnetic field. This modification, coupled with the polarization introduced by the Brewster windows, allows one to change the intracavity losses. The Kerr cell is modulated at a frequency determined by the operating conditions of the laser. When the modulation is small, the losses within the cavity are small, and the laser output tracks the input from the signal generator. The input signal (from the signal generator) and the output signal (the measured laser intensity) are both recorded in a computer (C). When the modulation crosses a threshold, the laser output can no longer track the signal input.

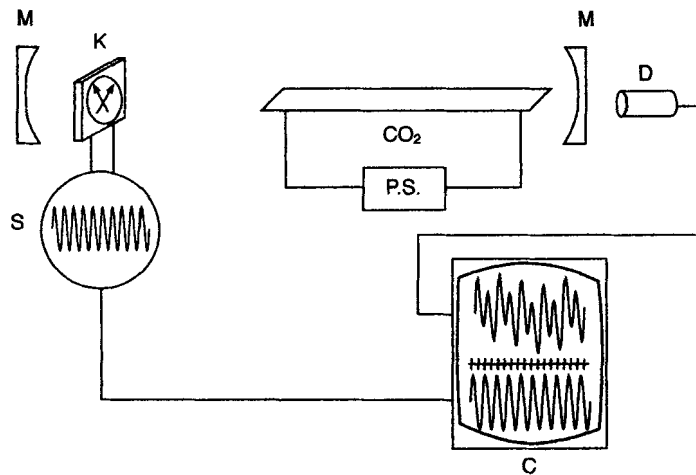


Fig. 1.1 This schematic representation of a laser with modulated losses shows the carbon dioxide tube (CO₂); power source (P.S.); mirrors (M); Kerr cell (K); signal generator (S); detector (D); and computer, oscilloscope, and recorder (C). A variable electric field across the Kerr cell rotates its polarization direction and modulates the electric field amplitude within the cavity.

At first every other output peak has the same height, then every fourth peak, then every eighth peak, and so on.

In Fig. 1.2 we present some of the recorded and processed signals from this part of the period-doubling cascade and beyond [6]. The signals were recorded under different operating conditions and are displayed in five lines, as follows: (a) period 1; (b) period 2; (c) period 4; (d) period 8; (e) chaos. Each of the four columns presents a different representation of the data. In the first column the intensity output is displayed as a function of time. In this presentation the period-1 and period-2 behaviors are clear but the higher-period behavior is not.

The second column displays a projection of the dynamics into a two-dimensional plane, the dI/dt vs. $I(t)$ plane. In this projection, periodic orbits appear as closed loops (deformed circles) which go around once, twice, four times, . . . before closing. In this presentation the behavior of periods 1, 2, and 4 is clear. Period 8 and chaotic behavior is less clear. The third column displays the power spectrum. Not only is the periodic behavior clear from this display, but the relative intensity of the various harmonics is also evident. Chaotic behavior is manifest in the broadband power spectrum. Finally, the last column displays a stroboscopic sampling of the output. In this sampling technique, the output intensity is recorded each time the input signal reaches a maximum (or some fixed phase with respect to the maximum). There is one sample per cycle. In period-1 behavior, all samples have the same value. In period-2 behavior, every other sample has the same value. The stroboscopic display

clearly distinguishes between periods 1, 2, 4, and 8. It also distinguishes periodic behavior from chaotic behavior. The stroboscopic sampling technique is equivalent to the construction of a Poincaré section for this periodically driven dynamical system. All four of these display modalities are available in real time, during the experiment.

The laser with modulated losses has been studied extensively both experimentally [3–9] and theoretically [10–12]. The rate equations governing the laser intensity I and the population inversion N are

$$\begin{aligned}\frac{dI}{dt} &= -k_0 I [(1 - N) + m \cos(\omega t)] \\ \frac{dN}{dt} &= -\gamma [(N - N_0) + (N_0 - 1)IN]\end{aligned}\quad (1.1)$$

Here m and ω are the modulation amplitude and angular frequency, respectively, of the signal to the Kerr cell; N_0 is the pump parameter, normalized to $N_0 = 1$ at the threshold for laser activity; and k_0 and γ are loss rates. In dimensionless, scaled form this equation is

$$\begin{aligned}\frac{du}{d\tau} &= [z - A \cos(\Omega\tau)]u \\ \frac{dz}{d\tau} &= (1 - \epsilon_1 z) - (1 + \epsilon_2 z)u\end{aligned}\quad (1.2)$$

The scaled variables are $u = I$, $z = k_0 \kappa (N - 1)$, $t = \kappa \tau$, $A = k_0 m$, $\epsilon_1 = 1/\kappa k_0$, and $\epsilon_2 = 1/\gamma k_0 (N_0 - 1)$. The bifurcation behavior exhibited by the simple models (1.1) and (1.2) is qualitatively, if not quantitatively, in agreement with the experimentally observed behavior of this laser.

A bifurcation diagram for the laser model (1.2) is shown in Fig. 1.3. The bifurcation diagram is constructed by varying the modulation amplitude A and keeping all other parameters fixed. The overall structures of the bifurcation diagrams are similar to experimentally observed bifurcation diagrams.

This figure shows that a period-1 solution exists above the laser threshold ($N_0 > 1$) for $A = 0$ and remains stable as A is increased until $A \sim 0.8$. It becomes unstable above $A \sim 0.8$, with a stable period-2 orbit emerging from it in a period-doubling bifurcation. Contrary to what might be expected, this is not the early stage of a period-doubling cascade, for the period-2 orbit is annihilated at $A \sim 0.85$ in an inverse saddle-node bifurcation with a period-2 regular saddle. This saddle-node bifurcation destroys the basin of attraction of the period-2 orbit. Any point in that basin is dumped into the basin of a period $4 = 2 \times 2^1$ orbit, even though there are two other coexisting basins of attraction for stable orbits of periods $6 = 3 \times 2^1$ and 4 at this value of A .

Subharmonics of period n (P_n , $n \geq 2$) are created in saddle-node bifurcations at increasing values of A and I (P_2 at $A \sim 0.1$, P_3 at $A \sim 0.3$, P_4 at $A \sim 0.7$, P_5 and higher shown in the inset). All subharmonics in this series up to period $n = 11$ have been seen both experimentally and in simulations of (1.2). The evolution (*perestroika* [13]) of each of these subharmonics follows a standard scenario as T increases [14]: